J Therm Anal Calorim (2010) 99:83–86
DOI 10.1007/s10973-009-0564-8

Magnetic and thermal analysis of MFe$_2$O$_4$ (M = Co, Mn, Zn) nanoparticles

Yuko Ichiyanagi · Yuki Moro · Hikaru Katayanagi · Shinji Kimura · Daiki Shigeoka · Tomoyuki Hiroki · Toshiyuki Mashino

Japan Symposium 2008

Abstract Magnetic nanoparticles were prepared by a wet chemical method. Precursors of MFe$_2$O$_4$ (M = Co, Mn, Zn) were prepared from a mixture of metal chloride and metasilicate nonahydrate aqueous solutions. The precipitates obtained in the wet chemical method were calcined to obtain MFe$_2$O$_4$ nanoparticles encapsulated by amorphous SiO$_2$. The blocking temperatures T_B's were between 20 and 320 K, in this temperature range, the anisotropy energy of the particles decreased below their thermal energy. T_B increased with the particle size. In order to clarify the nanoparticle formation process, differential thermal analysis and thermogravimetric (TG-DTA) measurements were performed for the as-prepared samples.

Keywords Magnetic nanoparticles · Magnetization · TG-DTA measurement · Thermal fluctuation

Introduction

Magnetic nanoparticles are attracting considerable attention because of their potential use in magnetic recording media, magnetic fluids, catalysis agents, and biomedical equipment. In particular, ferrite nanoparticles are appropriate for use in hyperthermia agents because of their relatively large saturation magnetization at room temperature [1].

One of the authors has successfully produced magnetic nanoparticles encapsulated in amorphous SiO$_2$ and has reported their magnetic and thermal [2–7] properties. We have also suggested that these magnetic nanoparticles can be used in biomedical applications for producing functional magnetic nanoparticles [8, 9]. Ni–Zn ferrite nanoparticles have been reported to display magnetic properties and thermal fluctuation that depend on the particle size [6]. The Co-ferrite (CoFe$_2$O$_4$) bulk crystal is known to have an inverse spinel structure with 80% of the Co^{2+} ions being positioned at tetrahedral B sites [10]. The CoFe$_2$O$_4$ bulk crystal shows a saturation magnetization of 3.9 μ_B, and it has a Curie temperature of 520 K.

A bulk crystal of MnFe$_2$O$_4$ has a spinel structure with 93% of the Mn^{2+} ions being located at the tetrahedral A sites [11, 12]; however, the distribution of the Mn^{2+} ions can vary with the preparation method. The MnFe$_2$O$_4$ bulk crystal shows the largest saturation magnetization among ferrite group compounds, exhibiting a value of 4.73 μ_B [13], and it has a Curie temperature of 573 K. ZnFe$_2$O$_4$ is known to be antiferromagnetic [14].

In this study, CoFe$_2$O$_4$ nanoparticles with sizes ranging between 2.1 and 30.7 nm and Mn$_{0.5}$Zn$_{0.5}$Fe$_2$O$_4$ nanoparticles with sizes ranging between 2.1 and 30.7 nm are prepared. Magnetic particles whose diameter is below a critical diameter cannot support more than one domain and thus form a single domain. The critical diameter of commonly used materials is typically between 10 and 100 nm [15–18]. Single-domain ferromagnetic particles are characterized by a temporary large coercive force for a certain domain size; however, in the case of small particles, the coercive force is not always observed [19] because the magnetic spins of the particles fluctuate with the thermal energy.

Y. Ichiyanagi (✉) · Y. Moro · H. Katayanagi · S. Kimura · D. Shigeoka · T. Hiroki · T. Mashino
Department of Physics, Graduate School of Engineering, Yokohama National University, 79-5 Tokiwadai, Hodogaya-ku, Yokohama 240-8501, Japan
e-mail: yuko@ynu.ac.jp

Y. Ichiyanagi
Japan Science and Technology Agency, Precursory Research for Embryonic Science and Technology, 5 Sanbanchou, Chiyoda-ku, Tokyo 102-0075, Japan

Experimental

M-ferrite (MFe_2O_4) nanoparticles were produced by mixing aqueous solutions of $MCl_2{\cdot}nH_2O$, $FeCl_2{\cdot}4H_2O$, and $Na_2SiO_3{\cdot}9H_2O$. Aqueous solutions of $ZnCl_2$ were also added in some cases. The mole ratio of the prepared reagent was M:Si = 1:1. The obtained precipitates were washed several times with distilled water and dried at about 350 K in a thermostat. The as-prepared samples were subjected to heat treatment in a furnace in air or in an Ar atmosphere at annealing temperatures of 873 to 1,123 K. Each sample was examined by using CuKα X-ray powder diffraction ($\lambda = 0.154$ nm). Particle sizes were estimated by examining X-ray diffraction patterns and confirmed by transmission electron microscope (TEM, JEM 2000FXII). Magnetization measurements were performed using a SQUID magnetometer (Quantum Design, MPMS) under a magnetic field of $\pm$50 kOe at temperatures from 2 to 300 K. Differential thermal analysis and thermogravimetric (TG-DTA, RIGAKU TAS-100) measurements were carried out for the as-prepared samples.

Results and discussion

X-ray diffraction and TEM images

Figure 1 shows the CuKα X-ray powder diffraction patterns of $CoFe_2O_4$ (a) and $Mn_{0.5}Zn_{0.5}Fe_2O_4$ (b) annealed at different temperatures. $CoFe_2O_4$ nanoparticles were annealed in air and $Mn_{0.5}Zn_{0.5}Fe_2O_4$ nanoparticles were annealed in an Ar atmosphere. Around $2\theta = 23°$, a broad peak of amorphous SiO_2 was observed. The peaks become sharper as the annealing temperature increased. This phenomenon reflects the typical transformation occurring during crystal growth. In all cases, a spinel structure with a lattice constant of 0.839 nm for $CoFe_2O_4$ and 0.848 nm for $Mn_{0.5}Zn_{0.5}Fe_2O_4$ is confirmed, even though the patterns of the samples annealed at low temperatures are fairly broad due to the amorphous state of the samples. A single spinel phase of $CoFe_2O_4$ and $Mn_{0.5}Zn_{0.5}Fe_2O_4$ in amorphous SiO_2 is observed in the samples. The particle diameter is estimated from the broadening of the diffraction peaks by using the Scherrer formula: the estimated diameters are between 2.1 and 30 nm, depending on the annealing temperature. These sizes are confirmed by the TEM image. Two examples are shown in Fig. 2. The relationship between the annealing temperature and the particle diameter size is displayed in Fig. 3.

Magnetization measurements

Magnetization measurements were performed using the SQUID magnetometer under an external field of 50 to $-$50 kOe at temperatures of 5–300 K. Figure 4 shows the temperature dependence of both the field-cooled (FC) (closed marks) and the zero-field-cooled (ZFC) (open marks) magnetization for samples with particle diameters of 2.8, 3.2, 4.1, and 4.9 nm for $CoFe_2O_4$ (Fig. 4a) and 2.1, 3.5, 4.5, 6.5, and 18.0 nm for $Mn_{0.5}Zn_{0.5}Fe_2O_4$ (Fig. 4b) under an external field of 100 Oe. The bifurcation temperature of the FC-ZFC magnetization can be defined as the blocking temperature T_B. The nanoparticles prepared in this study are considered to have a single domain, and magnetic spins in the particles become unstable during thermal energy fluctuations. Above T_B, thermal energy becomes larger than anisotropy energy, and magnetic spins fluctuate with the thermal energy and behave superparamagnetically. T_B is

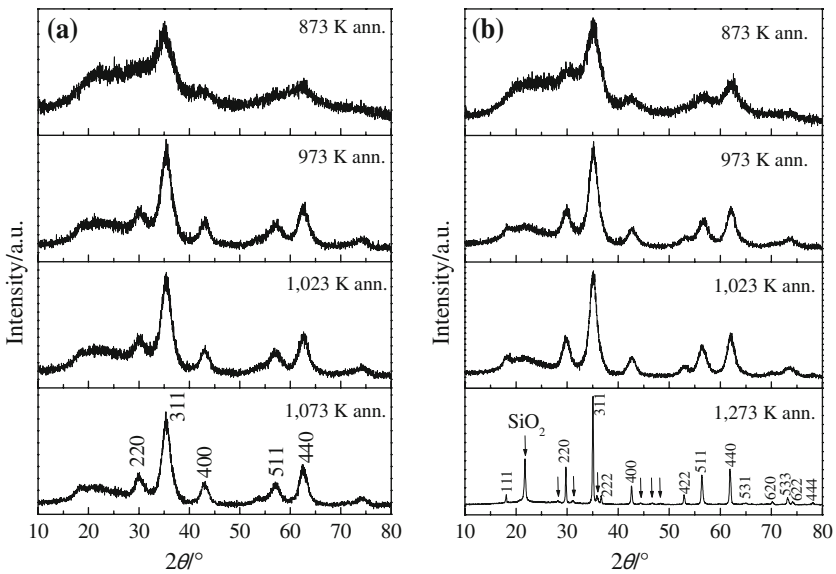

Fig. 1 Powder X-ray diffraction patterns for $CoFe_2O_4$ annealed in air (**a**) and $Mn_{0.5}Zn_{0.5}Fe_2O_4$ annealed in Ar (**b**) nanoparticles

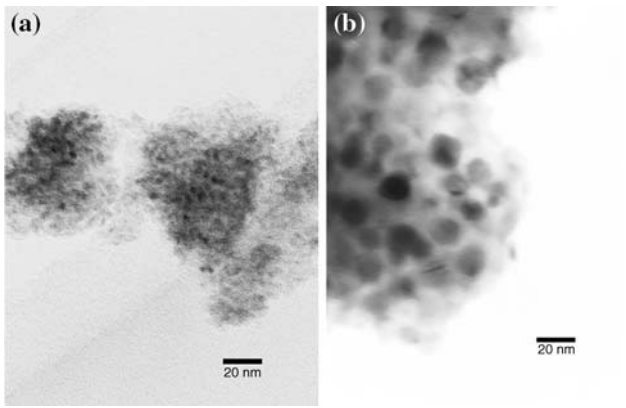

Fig. 2 TEM images of 4.1 nm $CoFe_2O_4$ nanoparticles (**a**) and 18 nm $Mn_{0.5}Zn_{0.5}Fe_2O_4$ nanoparticles (**b**) in amorphous SiO_2

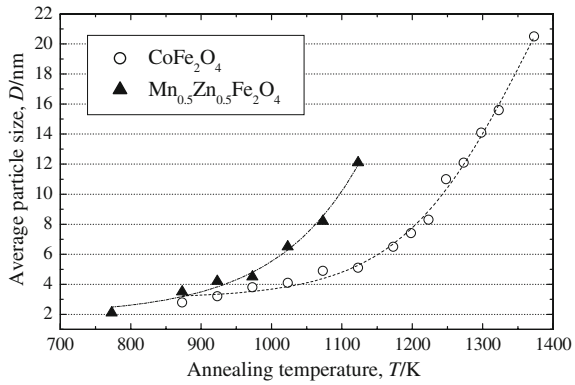

Fig. 3 Relationship between annealing temperature and particle diameter for $CoFe_2O_4$ and $Mn_{0.5}Zn_{0.5}Fe_2O_4$

observed to be between 20 and 370 K. Below T_B, ferromagnetic behavior is also observed. With an increase in the particle size, the magnetization and T_B increase. The particle sizes and corresponding T_B values are listed in Table 1. If we further define the peak temperature of ZFC magnetization as average blocking temperature $T_{B(ave)}$, and the bifurcation temperature of the FC-ZFC magnetization as maximum blocking temperature $T_{B(max)}$, sometimes, in case of particle size distribution, these two temperatures have great differences. A $CoFe_2O_4$ particle of 4.1 nm exhibits a little bit higher blocking temperature than that of 4.9 nm, such a phenomena could be explained in that size distribution of the particle is rather large.

The relation between the anisotropy energy and thermal fluctuation is given by the following formula:

$$Kv = k_B T \quad (1)$$

where K is the anisotropy constant, v is the particle volume, and k_B is the Boltzmann constant. If we simply apply this relation, we can roughly estimate T_B value. Assuming $K \approx 2 \times 10^5$ J m^{-3}, for $CoFe_2O_4$, the formula gives a T_B

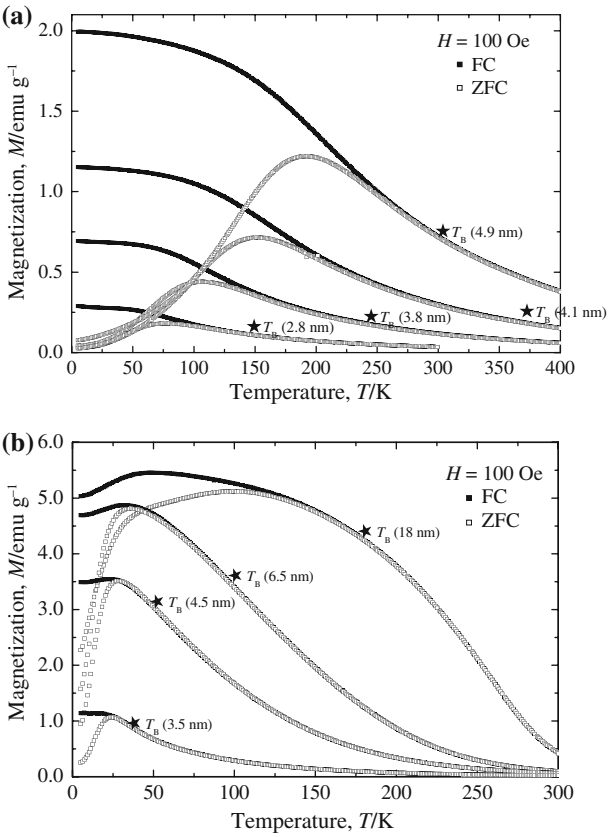

Fig. 4 Temperature dependence of FC (*closed marks*) and ZFC (*open marks*) magnetization in $CoFe_2O_4$ nanoparticles (**a**) and $Mn_{0.5}Zn_{0.5}Fe_2O_4$ nanoparticles (**b**)

Table 1 Relation between the particle sizes and blocking temperatures for $CoFe_2O_4$ (a) and $MnZnFe_2O_4$ (b)

(a)		(b)	
D/nm	T_B/K	D/nm	T_B/K
4.9	312	18.0	177
4.1	372	6.5	102
3.2	254	4.5	51
2.8	154	3.5	33

value of about 400 K for a particle diameter of 4 nm, even though the exact anisotropy constant is unknown. We do not have any data of K for $Mn_{0.5}Zn_{0.5}Fe_2O_4$, however, anisotropy energy is considered to be lower because Zn ions are nonmagnetic.

TG-DTA measurements

In order to clarify the nanoparticle formation process and heat-treatment effect on the nanoparticles, TG-DTA measurements were carried out in air using a Rigaku TAS-100 instrument. In the TG curve, mass loss due to dehydration was observed at temperatures above 370 K, after which the

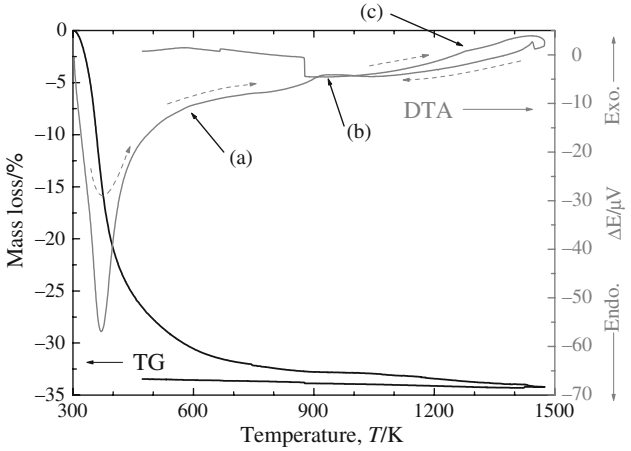

Fig. 5 TG-DTA curves of as-prepared $MnZnFe_2O_4$ nanoparticles under air in the temperature range from room temperature to 1,500 K

sample mass gradually decreased with an increase in the temperature up to 1,500 K, as shown in Fig. 5 for $Mn_{0.5}Zn_{0.5}Fe_2O_4$.

Figure 5 also shows the DTA curve for the as-prepared samples of $Mn_{0.5}Zn_{0.5}Fe_2O_4$ from room temperature to 1,500 K. It is observed that a sharp endothermic peak corresponding to the above-mentioned dehydration phenomenon occurs at around 370 K. Particles gradually begin to grow at around 600 K (Fig. 5a), then an exothermic peak is observed at around 950 K (Fig. 5b). This small peak can possibly be attributed to the crystallization of the amorphous as-prepared sample at that temperature. This explanation can be supported by that a spinel phase can be clearly observed by the powder X-ray diffraction patterns annealed at 973 K. The slight shoulder at around 1,270 K could be due to the crystallization of amorphous SiO_2 and the sudden aggregation of nanoparticles in the system (Fig. 5c). X-ray diffraction peaks annealed at 1,273 K are sharpened and peaks of crystallized SiO_2 are newly observed. The existence of an exothermic peak at 1,444 K has so far been unknown; however, Mn–Zn ferrite could have partially decomposed into other compounds such as α-Fe_2O_3.

Conclusions

Magnetization and TG-DTA measurements were performed for MFe_2O_4 (M = Co, Mn, Zn) nanoparticles encapsulated in amorphous SiO_2. The blocking temperature was observed to be between 20 and 370 K, at that temperature, magnetic spins in the particle fluctuated with the thermal energy. TG-DTA measurements indicated that the prepared precursor was first dehydrated, crystallized at around 980 K, and aggregated at about 1,270 K. These events were consistent with those indicated by powder X-ray diffraction patterns.

Acknowledgements This study was partially supported by Precursory Research for Embryonic Science and Technology of the Japan Science and Technology Agency, and a Promotion of Science Grant-in Aid for Scientific Research (No. 1851009100). I would like to thank Prof. T. Atake and Prof. H. Kawaji at the Tokyo Institute of Technology for the TG-DTA measurement and useful discussions.

References

1. Gorter EW. Saturation magnetization and crystal chemistry of ferromagnetic oxides (1. The spinel structure). Philips Res Rep. 1954;9:295–320.
2. Ichiyanagi Y, Uehashi T, Yamada S. Magnetic properties of Ni-Zn ferrite nanoparticles. Phys Stat Sol (c). 2004;1:3485–8.
3. Ichiyanagi Y, Yamada S. The size-dependent magnetic properties of Co_3O_4 nanoparticles. Polyhedron. 2005;24:2813–6.
4. Ichiyanagi Y, Kubota M. Magnetic properties of Mg-ferrite nanoparticles. J Magn Magn Mater. 2007;310:2378–80.
5. Ichiyanagi Y, Kimishima Y. Structural, magnetic and thermal characterization of Fe_2O_3 nanoparticles. J Therm Anal Calorim. 2002;69:919–23.
6. Ichiyanagi Y, Uehashi T. Thermal fluctuation and magnetization of Ni-Zn ferrite nanoparticles by particle size. J Therm Anal Calorim. 2005;81:541–4.
7. Kubota M, Kanazawa Y, Nasu K, Moritake S, Kawaji H, Atake T, et al. Effect of heat treatment on magnetic $MgFe_2O_4$ nanoparticles. J Therm Anal Calorim. 2008;92:461–3.
8. Ichiyanagi Y, Moritake S, Taira S, Setou M. Functional magnetic nanoparticles for medical application. J Magn Magn Mater. 2007;310:2877–9.
9. Moritake S, Taira S, Ichiyanagi Y, Morone N, Song SY, Hatanaka T, et al. Functionalized ultranano magnetic particles for an in vivo delivery system. J Nanosci Nanotech. 2007;7:937–44.
10. Satya Murthy NS, Natera MG, Begam RJ, Youssef SI. Ferrites, Porc Int Conf. 1971;60.
11. Pekeris CL. Ground state of two-electron atoms. Phys Rev. 1958;112:1649–58.
12. Pekeris CL. 1 ^{1}S, 2 ^{1}S, and 2 ^{3}S States of H- and of He. Phys Rev. 1962;126:1470–6.
13. Smit J, Wijn HPJ. Ferrite, Philips Tech Lib. 1959;278–83.
14. Jeyadevan B, Tohji K, Nakatuska K, Narayanasamy A. Irregular distribution of metal ions in ferrites prepared by co-precipitation technique structure analysis of Mn–Zn ferrite using extended X-ray absorption fine structure. J Magn Magn Mater. 2000;217:99–105.
15. Kittel C. Theory of the structure of ferromagnetic domains in films and small particles. Phys Rev. 1946;70:965–71.
16. Néel C. Compt Rend. 1947;224:1488.
17. Stoner EC, Wohlfarth EP. Interpretation of high coercivity in ferromagnetic materials. Nature. 1947;160:650.
18. Dunlop DJ. Philos Mag Ser. 1969;19:329.
19. Congiu F, Concas G, Ennas G, Falqui A, Fiorani D, Marongiu G, et al. Magnetic properties of nanocrystalline $CoFe_2O_4$ dispersed in amorphous silica. J Magn Magn Mater. 2004;272–276:1561–2.